WIND ENERGY
Wind Energ. (2009)
Published online. DOI: 10.1002/we.372

RESEARCH ARTICLE

A critical assessment of computer tools for calculating composite wind turbine blade properties

Hui Chen[1], Wenbin Yu[1] and Mark Capellaro[2]

[1] Department of Mechanical and Aerospace Engineering, Utah State University, Logan, UT 84322-4130, USA

[2] Endowed Chair of Wind Energy at the Institute for Aircraft Design, University Stuttgart, Allmandring 5B Stuttgart

ABSTRACT

The purpose of this paper is to critically assess several computer tools for calculating the inertial and structural properties of wind turbine blades. The theoretical foundation of each tool is briefly summarized, and the advantages and disadvantages of each tool are pointed out. Several benchmark examples, including a circular aluminium tube, a highly heterogeneous section, a multi-layer composite pipe, an isotropic blade-like section and a realistic composite wind turbine blade are used to evaluate the performance of different tools. Such a systematic and critical assessment provides guidance for wind turbine blade engineers to choose the right tool for effective design and analysis of wind turbine blades. Copyright © 2009 John Wiley & Sons, Ltd.

KEYWORDS
Composites; turbine blades; blade properties; VABS; PreComp; BPE; FAROB; CROSTAB

Correspondence
W. Yu, Mechanical and Aerospace Engineering, Utah State University, UMC 4130, Logan, UT 84322-4130, USA.
E-mail: wenbin.yu@usu.edu

Received 03 November 2008; Revised 06 August 2009; Accepted 07 August 2009

1. INTRODUCTION

Wind energy is becoming one of the most feasible and affordable renewable energy source available, as demonstrated by the fact that the installed capacity has increased by more than 24% annually in recent years and increased more than 10 times the wind power's share of the world's electricity generation since 1996.[1] Over the same period, the size of the average turbine has increased immensely. The economy of scale for larger turbines has been a key factor in lowering the cost of wind energy. Like other competing sources of electricity, wind power manufacturers are actively pursuing cost-saving measures to lower the costs. The trend in increased turbine size means an increase in the size of rotor blades. Manufacturers are now in serial production of 40-m blades for 2 MW and greater machines. Several turbine prototypes with diameters of 90–120 m have already been field tested.[2]

These huge sophisticated electromechanical systems pose a significant challenge for engineering design and analysis. Moreover, to reduce the excessive weight of large wind turbines and increase the fatigue life of the system, composite materials are used to make wind turbine components because of their high strength to weight ratios along with superb fatigue properties. The increasing application of composite materials further complicates the engineering design and analysis. The goal of design and analysis is to reliably model the behaviour of the wind turbine before any substantial cost is committed to building prototypes and testing. Although the current tools and methods have proven themselves by the low blade failure rate of the 90+GW capacity of wind turbines, manufacturers are constantly looking for analysis tools with better predictive capability to build the turbine more cost effectively.

Wind turbine blades are critical components of the wind turbine system, and how to design and build better turbine blades is an active field of research and development in the industry. Better designed blades will not only increase their own effectiveness, but could also result in substantial

savings for several major components such as the tower and the drive train, therefore, ultimately reducing the initial cost and operation cost of the whole system to improve the competitiveness of wind-generated electricity. Thus, reliable modelling of the blade is not only critical to the operation of the wind turbine, but is also considered as an indispensable part in the whole process of wind turbine design. The scale of today's wind turbine blades is now rendering the early trial-and-error intuition-based approaches as outdated. Engineers are relying on more reliable computer tools to analyse the blade structure in the early design process. To confidently design composite wind turbine blades, one must integrate both aerodynamic and structural concerns based on a rigorous treatment of the aeroelastic nature of the system. With the recent advances of computational hardware and software, it is possible to tackle this aeroelastic problem using Finite Element Analysis (FEA) coupled with Computational Fluid Dynamics (CFD).

The most labour and computationally intensive approach is to use the three-dimensional (3D) FEA based on brick elements. When performed correctly, this approach should provide the most accurate prediction. However, this approach requires detailed geometric and laminate layup information of the blade, making the modelling and computational costs too prohibitive for it to be an efficient approach for early design stages, including but not limited to, both conceptual design and preliminary design, not to mention that many structural details necessary for 3D modelling are not available until the late stages of the design process, after many design and analysis iterations.

Because the thickness of walls is usually small when compared with the chord length of the wind turbine blades, it is possible to use a two-dimensional (2D) FEA model based on laminated shell elements to simplify the analysis. This simplified 2D model, in comparison to the 3D FEA using brick elements, will dramatically reduce the required total number of degrees of freedom needed for modelling wind turbine blades to less than two orders of magnitude in comparsion to using 3D brick elements. However, it has been found that FEA, using shell elements with offset nodes, may result in very poor prediction for the shear stress; see, for example, the FEA of a simple isotropic thin-walled cylinder[3] and a composite box girder of a wind turbine blade.[4] Laminated shell elements are usually based on the Classical Laminate Theory (CLT), invoking the Kirchhoff–Love assumption. CLT ignores the transverse shear and normal stresses and strains which could be important for some failure mechanisms of the blade, such as delamination. Although shell elements with reference surface at the middle-surface can provide acceptable results for a simple cylinder with very thin walls, this approach leads to model discontinuity due to ply-drops and different thickness of the blade segments,[3] making it difficult to set up the model, interpret results and evaluate the accuracy of this method. For these reasons, a mid-thickness version of Sandia National Laboratories' wind turbine blade design and analysis code, NuMAD (Numerical Manufacturing And Design Tool) was developed as a front-end for the ANSYS commercial FEA code to simplify the process of generating the wind turbine blade model.[5]

It is well known that to accurately estimate the dynamic behaviour of the blades, we have to perform an aeroelastic analysis of the multi-body wind turbine system. Even if the aerodynamics part can be simplified, the multi-body dynamic behaviour must be simulated. The dynamic behaviour of the wind turbine can be performed with multi-body dynamics simulation codes such as the ADAMS commercial dynamic simulation code or more simplified codes such as the industry standard Blade Element Momentum (BEM) codes. The industry standard BEM codes (Flex5, Bladed) use a modal reduction method that simplifies the blades to a group of mode shapes and frequencies. This method has proven to be reasonably accurate and incredibly fast in calculating wind turbine dynamic responses. The mode shapes and frequencies can be directly obtained from FEA using brick elements or shell elements. However, because the wind turbine blades are very slender, with one dimension much larger than the other two, the first several elastic modes will demonstrate the so-called beam behaviour, including flapwise bending, edgewise bending and torsion. For this reason, the FEA based on brick elements or shell elements, although valuable for obtaining detailed stress distribution, are believed to be overkill for aeroelastic analysis of the multi-body system.[6] An alternative approach for simulating the multi-body dynamic behaviour is to model wind turbine blades as one-dimensional (1D) beams in a multi-body simulation code such as ADAMS. This approach is of particular value for introducing aeroelastic analysis and multi-flexible-body dynamic analysis[7] into the early design phases. The multi-body simulation codes are generally more accurate at the expense of greater computational time. With either dynamic simulation approach, the accuracy of the results is limited by the accuracy of the inertial and structural properties of the blade. Hence, the accurate and efficient calculation of wind turbine blade properties is critical throughout the design process.

Integrating accurate blade structural property calculation early into the wind turbine design process can help to detect serious aeromechanical problems before the design space is significantly narrowed. Structural optimization can be achieved through multiple iterations between the design modifications and comprehensive dynamic and aeroelastic simulations. It has also been shown that beam models of composite blades, if constructed appropriately, can achieve almost the same accuracy as 3D FEA using brick elements, for both global behaviour and pointwise 3D stress/strain distribution, at a cost of two to three orders of magnitude less.[8] Beam models such as the Euler–Bernoulli model and the Timoshenko model have been well established for a long time. How to evaluate sectional properties, including both structural and inertial properties, for composite beams with complex geometry has been an active research field in recent years.[9,10] Particularly

DOI: 10.1002/we

relevant to wind turbine blades, various approaches have been proposed in the literature and several tools are commonly used in the industry, including Pre-Processor for Computing Composite Blade Properties (PreComp),[11,12] Variational Asymptotic Beam Sectional Analysis (VABS),[8] FAROB (blade design tool from the Knowledge Centre Wind Turbine Materials WMC),[13] CROSTAB (Cross-sectional Stability of Anisotropic Blades)[14] and BPE (Blade Properties Extraction).[6] As the accuracy of blade properties directly affects the simulation of the statics and dynamics, and ultimately the performance and failure of the blade and the whole wind turbine system, it is crucial for us to have confidence in the calculated blade properties before we proceed to other calculations necessary for the design and analysis of the system.

In present work, a critical assessment of the computer tools currently used for calculating wind turbine blade properties in the industry is provided. First, the properties necessary for modelling turbine blades as beams are described. Then, several tools commonly used in the industry to obtain the blade properties are discussed in detail. The theoretical foundation of each tool is summarized along with the particular advantages and disadvantages. Several benchmark examples are used to evaluate the performance of different tools, including a circular aluminium tube, a highly heterogeneous section, a multilayer composite pipe, an isotropic blade-like section and a realistic composite wind turbine blade. The systematic and critical assessment will provide guidance for engineers to choose the right tool to effectively design and analyse wind turbine blades with confidence.

2. INERTIAL AND STRUCTURAL PROPERTIES OF COMPOSITE WIND TURBINE BLADES

A modern commercial wind turbine blade is a complex flexible structure that tapers along its length with possible initial twist and curvatures. The blade is built around a combination of aerodynamic profiles that vary along the blade. The aerodynamic shells are comprised of many layers of fibre-reinforced composite materials and foam. The structural reinforcement for many blades is based on a spar that runs along the length of the blade. The spar is usually built up with fibre reinforced composites to resist flapwise bending, and foam and fibre composite webs to resist edgewise bending, fatigue and buckling. To increase the clearance between the tower and blade, the blade tip sections are often angled away from the tower. Composite materials can also be strategically located along the length of the blade on the aerodynamic shells to reinforce the blade.

To accurately predict the behaviour of the complex wind turbine blade structure using a beam model, we need to find a way to reproduce as accurately as possible the energies, including both the kinetic energy and strain energy stored in the original 3D structure in a 1D format. Suppose V_1, V_2, V_3 represent three linear velocity components and Ω_1, Ω_2, Ω_3 represents three angular velocity components of any point in the beam reference, the kinetic energy density $\mathcal{K}$ of the beam can be written as:

$$\mathcal{K}=\frac{1}{2}\begin{Bmatrix} V_1 \\ V_2 \\ V_3 \\ \Omega_1 \\ \Omega_2 \\ \Omega_3 \end{Bmatrix}^T \begin{bmatrix} \mu & 0 & 0 & 0 & \mu x_{m3} & -\mu x_{m2} \\ 0 & \mu & 0 & -\mu x_{m3} & 0 & 0 \\ 0 & 0 & \mu & \mu x_{m2} & 0 & 0 \\ 0 & -\mu x_{m3} & \mu x_{m2} & i_{22}+i_{33} & 0 & 0 \\ \mu x_{m3} & 0 & 0 & 0 & i_{22} & -i_{23} \\ -\mu x_{m2} & 0 & 0 & 0 & -i_{23} & i_{33} \end{bmatrix} \begin{Bmatrix} V_1 \\ V_2 \\ V_3 \\ \Omega_1 \\ \Omega_2 \\ \Omega_3 \end{Bmatrix} \tag{1}$$

where μ is mass per unit length, (x_{m2}, x_{m3}) is the location of mass centre measured in the user-defined reference coordinate system, i_{22} is the mass moment of inertia about x_2 axis, i_{33} is the mass moment of inertia about x_3 axis and i_{23} is the product of inertia. Here, we choose x_1 along the beam reference line, and x_2 and x_3 for the coordinates in the cross-sectional plane, as sketched in Figure 1. It is noted here that it is common practice that the rotary inertia terms-associated bending are discarded in beam analysis using the Euler–Bernoulli model. If we choose the coordinate in such a way that x_1 is the locus of mass centres and x_2 and x_3 along the principal inertial axis, the 6×6 inertia matrix in equation (1) will become a diagonal matrix with μ, i_{22}, i_{33} to characterize the inertial properties of the cross-section. Hence, for an arbitrarily chosen coordinate system, we can also use these three values (μ, i_{22}, i_{33}) along with mass centre location (x_{m2}, x_{m3}), and the angle between the principal inertial axis and x_2 to replace the inertia matrix in equation (1). If the International Standard unit system is adopted (i.e., kg for mass and m for length), μ will have the unit of kg/m, i_{22} and i_{33} will have the unit of kg·m, and mass centre location x_{m2} and x_{m3} will have the unit of m. Oftentimes, the beam reference line is chosen based on engineering convenience. If we choose a different set of coordinates as the reference to express the kinetic energy, such as x_1^*, x_2^* and x_3^* parallel to x_1, x_2, x_3 in Figure 1, we need to carry out a proper transformation of the mass matrix in equation (1) which was originally calculated based on the unstarred coordinate system. Based on the definition of the linear and angular velocities,[9] we can derive the following relations:

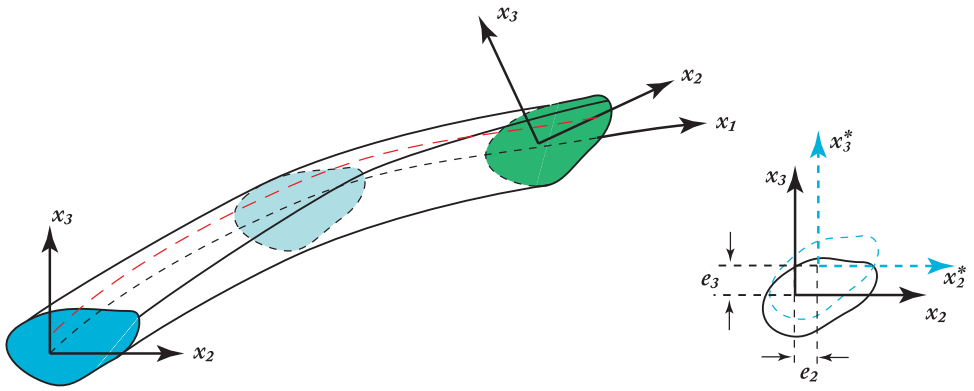

Figure 1. Coordinate system and sketch of a beam.

$$
\begin{aligned}
&V_1 = V_1^* - e_3\Omega_2^* + e_2\Omega_3^* \quad V_2 = V_2^* + e_3\Omega_1^* \\
&V_3 = V_3^* - e_2\Omega_1^* \quad \Omega_1 = \Omega_1^* \\
&\Omega_2 = \Omega_2^* \quad \Omega_3 = \Omega_3^*
\end{aligned} \tag{2}
$$

with the starred quantities denoting the velocity components in the starred coordinate system. This can also be written in the following matrix form as:

$$
\begin{Bmatrix} V_1 \\ V_2 \\ V_3 \\ \Omega_1 \\ \Omega_2 \\ \Omega_3 \end{Bmatrix} = \begin{bmatrix} 1 & 0 & 0 & 0 & -e_3 & e_2 \\ 0 & 1 & 0 & e_3 & 0 & 0 \\ 0 & 0 & 1 & -e_2 & 0 & 0 \\ 0 & 0 & 0 & 1 & 0 & 0 \\ 0 & 0 & 0 & 0 & 1 & 0 \\ 0 & 0 & 0 & 0 & 0 & 1 \end{bmatrix} \begin{Bmatrix} V_1^* \\ V_2^* \\ V_3^* \\ \Omega_1^* \\ \Omega_2^* \\ \Omega_3^* \end{Bmatrix} \tag{3}
$$

We know that the kinetic energy density of the blade, as a scalar, will remain invariant with respect to the choice of the coordinate systems. Substituting equation (3) into equation (1), we can express the kinetic energy in the starred coordinate system as:

with $x_{m3}^* = x_{m3} - e_3$, $x_{m2}^* = x_{m2} - e_2$ and $i_{11}^* = i_{22} + i_{33} + \mu(e_2^2 - 2x_{m2e2} + e_3^2 - 2e_3x_{m2})$.

The form of 1D strain energy depends on which model the beam theory is based on. For example, for the Euler–Bernoulli model which is capable of dealing with extension, torsion and bending in two directions, the strain energy can be written as:

$$
\mathcal{U} = \frac{1}{2} \begin{Bmatrix} \gamma_{11} \\ \kappa_1 \\ \kappa_2 \\ \kappa_3 \end{Bmatrix}^T \begin{bmatrix} EA & S_{12} & S_{13} & S_{14} \\ S_{12} & GJ & S_{23} & S_{24} \\ S_{13} & S_{23} & EI_{22} & S_{34} \\ S_{14} & S_{24} & S_{34} & EI_{33} \end{bmatrix} \begin{Bmatrix} \gamma_{11} \\ \kappa_1 \\ \kappa_2 \\ \kappa_3 \end{Bmatrix} \tag{5}
$$

where γ_{11}, κ_1, κ_2, κ_3 are the extensional strain, twist, bending curvatures about x_2 and x_3, respectively. The components of the 4×4 stiffness matrix in equation (5) depend on the choice of the beam coordinate system, initial curvatures/twist, as well as the geometry and material of the cross-section.[15] The diagonal terms EA, GJ, EI_{22}, EI_{33} are the extensional stiffness, the torsional stiffness and bending stiffness about x_2 and x_3, respectively. The off-diagonal terms represent the elastic couplings between different deformation modes. If the International Standard unit

$$
\mathcal{K} = \frac{1}{2} \begin{Bmatrix} V_1^* \\ V_2^* \\ V_3^* \\ \Omega_1^* \\ \Omega_2^* \\ \Omega_3^* \end{Bmatrix}^T \begin{bmatrix} \mu & 0 & 0 & 0 & \mu x_{m3}^* & -\mu x_{m2}^* \\ 0 & \mu & 0 & -\mu x_{m3}^* & 0 & 0 \\ 0 & 0 & \mu & \mu x_{m2}^* & 0 & 0 \\ 0 & -\mu x_{m3}^* & \mu x_{m2}^* & i_{11}^* & 0 & 0 \\ \mu x_{m3}^* & 0 & 0 & 0 & i_{22} + e_3(e_3 - 2x_{m3}) & (e_3x_{m2} + e_2x_{m3}^*)\mu - i_{23} \\ -\mu x_{m2}^* & 0 & 0 & 0 & (e_3x_{m2} + e_2x_{m3}^*)\mu - i_{23} & i_{33} + e_2(e_2 - 2x_{m2})\mu \end{bmatrix} \begin{Bmatrix} V_1^* \\ V_2^* \\ V_3^* \\ \Omega_1^* \\ \Omega_2^* \\ \Omega_3^* \end{Bmatrix} \tag{4}
$$

system is adopted (*i.e.*, N for force and m for length), EA will have the unit of N, GJ, EI_{22} and EI_{33} will have the unit of N·m^2. The coupling stiffness S_{12}, S_{13} and S_{14} will have the unit of N·m, and the coupling stiffness S_{23}, S_{24} and S_{34} will have the unit of N·m^2. We could also have the so-called tension centre (x_{t2}, x_{t3}) defined such that an axial force applied at this point will not introduce any bending. We can also find the so-called principal bending axis so that there is no coupling between two bending directions. For prismatic beams made of isotropic materials with the reference line located at the tension centres, and x_2 and x_3 aligned with the principal bending axes, the stiffness matrix is diagonal and the four deformation modes are completely decoupled. For more general cases such as initially curved or twisted composite beams, such decoupling is not possible and providing information regarding tension centre and principal bending axes is not as meaningful for composite beams as it is for isotropic beams. It is emphasized here that for general blades, the mass centre might not be the same as the tension centre, and the principal inertial axes might not be the same as the principal bending axes. In other words, it is impossible for us to choose a single coordinate system with the origin located both at the mass centre and the tension centre, x_2 and x_3 aligned with both the principal inertial axes and the principal bending axes. Also, it is important to repeat what has been pointed out in Hodges and Yu's study[16] that for accurate prediction using the Euler–Bernoulli beam model, it is necessary for the analyst to choose the reference along the locus of shear centres (x_{s2}, x_{s3}), particularly for torsional behaviour. For this very reason, providing the stiffness values for the Euler–Bernoulli model without providing the location of shear centre is not sufficient. For general composite beams, only the so-called generalized shear centre as defined in Hodges and Yu's study[16] will always exist.

One can also use the Timoshenko model which is capable of dealing with extension, torsion, bending in two directions and transverse shear in two directions to analyse the blade, the strain energy of which can be written as:

$$\mathcal{U}=\frac{1}{2}\begin{Bmatrix}\bar{\gamma}_{11}\\ 2\bar{\gamma}_{12}\\ 2\bar{\gamma}_{13}\\ \bar{\kappa}_1\\ \bar{\kappa}_2\\ \bar{\kappa}_3\end{Bmatrix}^T\begin{bmatrix}\bar{S}_{11}&\bar{S}_{12}&\bar{S}_{13}&\bar{S}_{14}&\bar{S}_{15}&\bar{S}_{16}\\ \bar{S}_{12}&\bar{S}_{22}&\bar{S}_{23}&\bar{S}_{24}&\bar{S}_{25}&\bar{S}_{26}\\ \bar{S}_{13}&\bar{S}_{23}&\bar{S}_{33}&\bar{S}_{34}&\bar{S}_{35}&\bar{S}_{36}\\ \bar{S}_{14}&\bar{S}_{24}&\bar{S}_{34}&\bar{S}_{44}&\bar{S}_{45}&\bar{S}_{46}\\ \bar{S}_{15}&\bar{S}_{25}&\bar{S}_{35}&\bar{S}_{45}&\bar{S}_{55}&\bar{S}_{56}\\ \bar{S}_{16}&\bar{S}_{26}&\bar{S}_{36}&\bar{S}_{46}&\bar{S}_{56}&\bar{S}_{66}\end{bmatrix}\begin{Bmatrix}\bar{\gamma}_{11}\\ 2\bar{\gamma}_{12}\\ 2\bar{\gamma}_{13}\\ \bar{\kappa}_1\\ \bar{\kappa}_2\\ \bar{\kappa}_3\end{Bmatrix} \tag{6}$$

where $2\bar{\gamma}_{12}$ and $2\bar{\gamma}_{13}$ are two transverse shear strains and bars are added to the symbols in equation (6) to indicate that they might be different from those in equation (5). The Timoshenko model provides better predictions for relatively shorter beams, particularly the dynamic behaviour, although it requires more degrees of freedom than the Euler–Bernoulli model. More significantly, the equations of the Timoshenko model are hyperbolic, a nature shared with the original 3D elasticity equations, which implies that it is capable of describing the effect of short pulse loading and wave propagation in the blade. Also, if one uses the Timoshenko model for the 1D beam analysis,[17] the analyst is free to choose an arbitrary reference line. Of course, when the coordinate system chosen for the 1D blade analysis is different from the coordinate system one used to calculate the stiffness properties, we need to transform the stiffness matrix properly. It can be shown that the relationship between the strain measures in the two coordinate systems as sketched in Figure 1 is exactly the same as those in equation (3),[9] that is:

$$\begin{Bmatrix}\bar{\gamma}_{11}\\ 2\bar{\gamma}_{12}\\ 2\bar{\gamma}_{13}\\ \bar{\kappa}_1\\ \bar{\kappa}_2\\ \bar{\kappa}_3\end{Bmatrix}=\begin{bmatrix}1&0&0&0&-e_3&e_2\\ 0&1&0&e_3&0&0\\ 0&0&1&-e_2&0&0\\ 0&0&0&1&0&0\\ 0&0&0&0&1&0\\ 0&0&0&0&0&1\end{bmatrix}\begin{Bmatrix}\bar{\gamma}^*_{11}\\ 2\bar{\gamma}^*_{12}\\ 2\bar{\gamma}^*_{13}\\ \bar{\kappa}^*_1\\ \bar{\kappa}^*_2\\ \bar{\kappa}^*_3\end{Bmatrix} \tag{7}$$

Using this relationship in Eq.(7), we can straightforwardly write out the stiffness matrix in the starred coordinate system. To transform the Euler–Bernoulli model into a different coordinate system, we just need to neglect the transverse shear strains in equation (7). As mentioned previously, to use the Euler–Bernoulli model, one must choose the shear centre as the reference. If a tool outputs a Euler–Bernoulli model at a different reference, we have to do the transformation. For example, if the stiffness coefficients for the Euler–Bernoulli model are given in terms of the tension centre, that is, S_{13} and S_{14} are zero in equation (5), then the Euler–Bernoulli model with the reference at the shear centre will be:

$$\mathcal{U}=\frac{1}{2}\begin{Bmatrix}\gamma^*_{11}\\ \kappa^*_1\\ \kappa^*_2\\ \kappa^*_3\end{Bmatrix}^T\begin{bmatrix}EA&S_{12}&-e_3EA&e_2EA\\ S_{12}&GJ&S_{23}-e_3S_{12}&S_{24}+e_2S_{12}\\ -e_3EA&S_{23}-e_3S_{12}&EI_{22}+e_3^2EA&S_{34}-e_2e_3EA\\ e_2EA&S_{24}+e_2S_{12}&S_{34}-e_2e_3EA&EI_{33}+e_2^2EA\end{bmatrix}\begin{Bmatrix}\gamma^*_{11}\\ \kappa^*_1\\ \kappa^*_2\\ \kappa^*_3\end{Bmatrix} \tag{8}$$

with e_2 and e_3 denoting offsets from the tension centre, positive along x_2 and x_3 directions, respectively.

The task of calculating the inertial properties in equation (1) and the structural properties in either equation (5) or equation (6) belongs to the domain of a cross-sectional analysis. Accurate evaluation of these properties is extremely important for successfully modeling wind turbine blades as beams for design and analysis purposes.

In fact, as pointed out by Ku *et al.*,[18] it is even possible to use the blade properties themselves as design variables, although this technique may appear too new to have found its way into the industry practice. It is emphasized here that most current wind turbine blade simulation tools only require a subset of the inertial properties and structural properties. For example, the current version of PHATAS[19] only requires mass per unit length (μ), bending stiffness (EI_{22}, EI_{33}, S_{34}) and torsional stiffness GJ. Currently, the torsional stiffness values are often ignored for blade design and analysis, mainly because most blades in operation are torsionally stiff and wind turbine airfoils have a low coefficient of moment. However, as the blade becomes larger, more flexible and more anisotropic, other inertial and structural properties such as the twist-bending coupling will be critically needed for better prediction.

3. DIFFERENT APPROACHES FOR CALCULATING BLADE PROPERTIES

In recent years, several approaches have been proposed for calculating the inertial and structural properties for wind turbine blades including PreComp,[12] VABS,[8] FAROB,[13] CROSTAB[14] and BPE.[6] It is pointed out that one can also use these tools to calculate the beam properties for other slender components in the wind turbine system, such as the tower or the drivetrain shaft, if the engineer chooses to model such components as beams. Without repeating the details of each tool that can be found in their relevant publications, we will only briefly summarize the theoretical foundation of each approach and point out the advantages and disadvantages of each approach in this section. A more extensive evaluation of each tool will be presented in the next section using some benchmark examples.

3.1. PreComp

PreComp is developed at the National Renewable Energy Laboratory.[11,12] In Bir's study[11], which can be considered as the precursor of the current version of PreComp, the bending stiffness EI_{22}, EI_{33} and S_{34} are calculated using the area-segments-based numerical integration. The torsional stiffness is computed by neglecting the effects of the warping functions altogether. The inertial properties are calculated by considering all the materials used in the blade construction, including surface coating and bonding adhesive. The current version of PreComp, as briefly described in Bir's article[12], is based on a novel approach that integrates a modified CLT with a shear-flow approach. In addition to thin-walled assumption and free warping assumption, it also invokes the following assumptions:

- Shear flow around each cell of the blade section is constant;
- There are no hoop stresses in any wall of the section;
- The blade is straight and the webs must be normal to the chord;
- Transverse shearing is negligible and the blade section is rigid in its own plane.

PreComp allows arbitrary cross-sectional geometry and material layups. It can predict the complete set of stiffness coefficients needed for the Euler–Bernoulli beam model in equation (5), and the inertial properties including mass per unit length, mass moments of inertia and the principal inertial axis. PreComp can also calculate the shear centre, tension centre and principal bending axis. The advantage of PreComp lies in its efficiency because it is not based on the finite element method. It is also general enough to deal most of wind turbine blades with very few restrictions. However, because of its adoption of oversimplified assumptions, there are some concerns about its accuracy in addition to its admitted approximation in shear centre calculations.

3.2. VABS

Under nearly two decades of support from the US Army and the National Rotorcraft Technology Centre, Hodges and his co-workers have developed VABS, a unique cross-sectional analysis tool capable of realistic modelling of initially curved and pre-twisted anisotropic blades with arbitrary sectional topology and material constructions.[9,16,20] The salient features of VABS are:

- *Use the variational asymptotic method to avoid* a priori *assumptions*, which are commonly invoked in other approaches, providing the most mathematical rigor and the best engineering generality and simplicity.
- *Decouple a 3D nonlinear problem into two sets of analyses*: a linear cross-sectional analysis over the cross-section and a geometrically exact beam analysis over the reference line. This allows the 1D beam analysis to be formulated exactly as a general continuum and confines all approximations to the cross-sectional analysis, the accuracy of which is guaranteed to be the best by the variational asymptotic method. Here, 'geometrically exact' refers to the fact that the finite rotation of the cross-sectional frame is treated exactly, without small-angle approximations.
- *Maintain the engineering simplicity and legacy* by repacking the refined, asymptotically correct functionals into common engineering models such as the Euler–Bernoulli model, the Timoshenko model or the Vlasov model.

VABS not only calculates the sectional properties compatible with linear and nonlinear beam analysis, but can also recover the pointwise distribution of the 3D displacement/stress/strain field. When compared with the FEA using 3D brick elements, two to three orders of magnitude in computing time can be saved by using VABS, with little loss

of the accuracy.[17] It should be emphasized, however, that VABS can only provide accurate 3D fields away from beam boundaries, concentrated loads and sudden changes in the cross-sectional geometry along the span. The detailed 3D information in these areas can only be provided by a 3D FEA. VABS can also handle hygrothermal effects of conventional composites, piezoelectric effects of smart material.[21–24] The advantages of VABS over other technologies are demonstrated by its virtues of being general-purposed, accurate and robust. However, VABS requires a finite element discretization of the cross-section, and it is very tedious to generate VABS input files for realistic rotor blades made of hundreds of composite layers. Very recently, a design-driven pre-processing computer program, PreVABS, has been developed for efficiently generating VABS inputs for realistic blades by directly using the design parameters such as CAD geometric outputs and the spanwise- and chordwise-varying cross-sectional laminate lay-up schema. PreVABS can handle complex blade configurations, including both symmetric and asymmetric airfoil profiles, both spanwisely and chordwisely varying lamina schema. VABS, powered by PreVABS, can easily provide an efficient high-fidelity analysis for real blades with hundreds of composite layers with a model setup effort similar to that of PreComp.

3.3. FAROB

The FAROB code is a module of the FOCUS package developed at the Dutch Knowledge Centre Wind Turbine Materials and Construction, the main analysis engine for the structural design of wind turbine blades. FAROB assumes the blade is formed by a number of thin-walled, homogenized, multi-layer segments, with each segment characterized by its Young's modulus, shear modulus and mass density.[13] These coefficients are evaluated in terms of the properties of each individual ply using the CLT. The bending stiffness EI_{22}, EI_{33} and S_{34} are calculated as summation of modulus weighted second-order moments of inertia. The torsional stiffness and shear centre are calculated by assuming constant shear flow for each cell following the traditional method used for thin-walled beams made of isotropic, homogeneous materials. The advantage of the FAROB code is that it is very efficient, because all of the calculation is based on analytical formulas, and it also incorporates thermal expansion coefficients and hygroscopic swelling coefficient into its calculation so that the environmental effects on the blade properties are also captured. FAROB is fully integrated into the FOCUS package, enabling the designer to build up a composite blade using the geometry of the airfoils, material properties and laminate schedule to calculate the blade properties. FAROB results can then be used in the full turbine system dynamic simulation code PHATAS, also part of the FOCUS code package. However, FAROB only produces a subset of the inertial and structural properties of the section. Particularly, it misses the increasingly important coupling terms between twist and other deformation modes and as well as the location of the shear center.

3.4. CROSTAB

In CROSTAB, a code developed at the Energy Research Centre of the Netherlands, a blade section is modelled as a layered shell structure which can have several webs, each forming a closed cell. It is assumed that the walls carry only in-plane loads. The sectional properties are calculated based on the inverse of the membrane stiffness matrix of the CLT, neglecting the bending and torsional stiffness of the walls. The shear flow effects are also considered in the calculation of extension and bending stiffness. Hence, CROSTAB can provide the complete set of sectional properties of the Euler–Bernoulli beam model, including all the coupling terms. Besides its efficiency due to its simplified analytical formulation, the advantage of CROSTAB also lies on the fact that it treats the composite materials more rigorously than FAROB so that the complete set of coupling terms can be calculated. However, it cannot calculate the shear centre location, which is indispensable for one to use the Euler–Bernoulli beam model. Also, for thick composites, the assumption introduced by the omission of the bending and torsional stiffness of the laminated walls may generate further limitations.

3.5. BPE

BPE,[6,25] developed by Global Energy Concepts and the Sandia National Laboratories, uses FEA displacement results from a suite of unit tip load solutions to extract the stiffness matrices for the equivalent beam elements. It is currently a module of NuMAD.[5] The basic concept is to obtain the beam displacements and rotations from the displacements of the FEA model under six linearly independent load cases of unit forces/moments. The deflections, and hence, beam properties can be calculated anywhere along the blade axis. The FEA analysis can either use 3D brick elements or 2D shell elements. In principle, the FEA model using 3D brick elements should be able to capture all the 3D information and repack it into a 1D form of a corresponding beam model. However, there are seemingly several challenges facing this approach. Firstly, the application of the unit forces/moments must ensure that the boundary layer effects are minimized. Secondly, it is very difficult to calculate the equivalent beam displacements and rotations from the 3D displacement field if FEA uses brick elements, or from the 2D displacement and rotation field if FEA uses shell elements. The difficulty in selecting the right set of nodes to determine the sectional displacement is a problem. The least square approach used in Malcolm and Laird's study[6] to obtain three displacements and three rotations of the equivalent beam element, out of possibly millions of nodal displacements, might be too rigid to obtain meaningful results because we are seeking six numbers to provide an optimal match to the original

displacement/rotation field described by millions of nodal values. Thirdly, the sectional properties will depend on the size of the blade segment one chooses to perform the FEA. For example, the stiffness coefficients may vary significantly in some cases as the length of the segment changes. Under some extreme situations, this variation may even lead to singular stiffness matrix[6]. Without a rigorous treatment of these three challenges, this approach will have difficulty to provide reliable predictions for the blade properties, particularly the torsional stiffness. As commented in Bir's study[12], BPE may overestimate the torsional stiffness 50–80 times because of its poor treatment of warping effects. The advantage of BPE, if the three aforementioned challenges could be mathematically resolved, is that it can include all the 3D details, including tapering, into a 1D beam element. Since it depends on a FEA, using either 3D brick elements or 2D shell elements, this approach will be more labour-intensive and computational-expensive in comparison to the other approaches.

3.6. Overall assessment

Although it is difficult to provide a conclusive statement about each tool purely based its publications, a qualitative assessment regarding their theoretical foundations and their functionalities can be provided. PreComp, VABS, FAROB and CROSTAB are cross-sectional analysis tools, while BPE relies on a FEA of a blade segment. For this very reason, even if the FEA uses 2D elements, BPE cannot compete with the other four cross-sectional tools as far as efficiency is concerned. If one can resolve the three aforementioned challenges facing the concept of BPE method, it should be able to provide accurate predictions for sectional properties, although how accurate it is can only be disclosed by comparing its performance against other tools. Unfortunately, the authors could not access the BPE results at the time of writing.

Among the four cross-sectional analysis tools, it seems the theory of FAROB is the most rudimentary as it treats each segment as isotropic and homogenous by homogenizing each multi-layer anisotropic segment. The theory of CROSTAB will be a little bit more sophisticated than FAROB by considering the anisotropy of individual layers although the bending and torsional stiffness of the walls are neglected. Although it is hard to assess the theory of PreComp because of its very limited description, it does show a level of sophistication with its ability to calculate the shear centre of an arbitrary composite cross-section. PreComp can provide the beam information necessary for an Euler–Bernoulli element, but it cannot provide a Timoshenko model or a Vlasov model.

VABS has a unique mathematical foundation which is far more sophisticated than the other tools. As far as efficiency is concerned, PreComp, FAROB and CROSTAB should be similar, because their calculations are based on analytical formulas, and should be more efficient than VABS which is based on a 2D FEA of the cross-section. As far as functionalities are concerned, usually it is not that difficult for any tool to calculate the inertial properties, including mass per unit length, mass moments of inertia and principal inertial axis. For structural properties, VABS can provide the most amount of information for a given cross-section, including Euler–Bernoulli model, Timoshenko model and Vlasov model, and characteristic centres including mass centre, shear centre and tension centre. The BPE method can only provide a Timoshenko model for the blade, along with shear centre and tension centre. CROSTAB can provide the structural properties for the Euler–Bernoulli model with the shear centre location. FAROB provides the principal bending and torsional stiffness values along with mass per unit length and mass centre. Among all the cross-sectional analysis tools, only VABS can accurately recover the 3D displacement, stress and strain field, comparable to a 3D FEA using brick elements.

4. ASSESSMENT EXAMPLES

This section presents a detailed and systematic assessment of several wind turbine blade design and analysis tools, including PreComp, VABS, FAROB and CROSTAB. Various examples of isotropic and composite sections with different geometry and laminate layup schemas, including a circular aluminium tube, a highly heterogeneous section, a multi-layer composite pipe, an isotropic blade-like section and a realistic composite wind turbine blade, are analysed. The resulting sectional properties such as the mass and stiffness coefficients, the locations of the mass centre and the shear centre are compared with each other to assess accuracy and limitations of these tools. Although VABS can provide various common engineering beam models such as the Euler–Bernoulli model, the Timoshenko model and the Vlasov model for composite blades, only the sectional properties for the Euler–Bernoulli model are used to facilitate our comparison with other three tools, which can only provide the Euler–Bernoulli model. Nevertheless, for reference, the VABS Timoshenko stiffness matrix calculated with respect to the origin of the user-defined coordinate system is also listed for each example. As pointed out by Hodges and Yu[16], when the Euler-Bernoulli beam model is used, an analyst must choose the reference line along the generalized shear centres for a reliable prediction of the behaviour of the wind turbine blades. Hence, the shear centre location is also provided for cases where it is not at the origin of the coordinate system. The inertial properties provided for the following examples are referred to the principal inertial axes at the mass centre. The structural properties are referred to the shear centre with axes parallel to the user defined axis x_2 and axis x_3.

For composite beams, the accuracy of the sectional properties predicted by different methods strongly depends on various cross-sectional parameters including:

DOI: 10.1002/we

- lamination parameters (viz. number of layers, stacking sequence, degree of anisotropy and fibre orientations);
- geometric parameters (viz. the thickness to blade chord length ratio, sectional topology and initial curvatures and twist).

Because of the large number of these parameters and the fact that analytical solutions are only obtainable for isotropic sections with simple geometry, in this work analytical results are only obtained for isotropic cases and numerical studies are performed for more complex composite sections. The analytical method used in this article is either based on the Elasticity theory or based on the thin-walled theory readily available in textbooks on isotropic beam theories.[26]

4.1. A Circular Aluminium Tube

A schematic of a circular tube made of aluminium is depicted in Figure 2, where the circular cylinder has a radius of $R = 0.3$ m with the Young's modulus of $E = 73$ GPa, Poison's ratio of $\nu = 0.33$ and density of $\rho = 2800$ kg/m^3. With the origin at the centre, only diagonal terms of the cross-sectional stiffness and mass matrix are not zero. Table I lists the results obtained by using PreComp, VABS, FAROB, CROSTAB and the Elasticity theory. For PreComp the section is discretized with 20 layers and 100 segments along the circumference while for VABS the cross-sectional model uses 1216 8-node quadrilateral elements. No discretization is needed as inputs for FAROB and CROSTAB. The unit listed for each quantity is according to the International Standard and will remain the same for all the other examples. The relative errors of different results with respect to the Elasticity theory are plotted in Figure 3 as a function of the ratio of the thickness to the chord length (CL), $t/(\mathrm{CL}) = t/2R$. The relative error is defined as $\left|\frac{X - X_{\mathrm{exact}}}{X_{\mathrm{exact}}}\right| \times 100\%$, where X is a specific

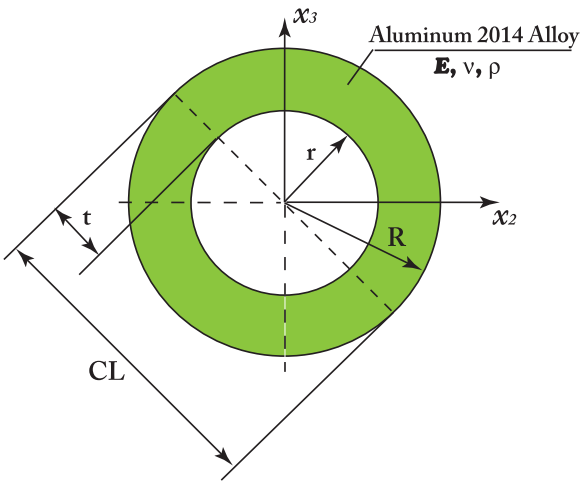

Figure 2. Schematic of a cylindrical aluminium tube.

Table I. Sectional properties of a circular aluminium tube.

$t/2R$	Method	EA	$EI_{22} = EI_{33}$	GJ	$i_{22} = i_{33}$	μ
1/15	PreComp	5.500E+09	2.152E+08	1.614E+08	8.264E+00	2.110E+02
	VABS	5.128E+09	2.022E+08	1.544E+08	7.755E+00	1.967E+02
	FAROB	/	2.024E+08	1.413E+08	/	1.970E+02
	CROSTAB	5.138E+09	2.014E+08	1.227E+08	7.726E+00	1.971E+02
	Elasticity	5.137E+09	2.024E+08	1.553E+08	7.763E+00	1.970E+02
1/7.5	PreComp	1.100E+10	3.733E+08	2.783E+08	1.434E+01	4.219E+02
	VABS	9.523E+09	3.298E+08	2.518E+08	1.265E+01	3.653E+02
	FAROB	/	3.301E+08	2.101E+08	/	3.659E+02
	CROSTAB	9.544E+09	3.224E+08	1.168E+08	1.238E+01	3.661E+02
	Elasticity	9.540E+09	3.301E+08	2.532E+08	1.266E+01	3.659E+02
1/5	PreComp	1.650E+10	4.832E+08	3.556E+08	1.856E+01	6.329E+02
	VABS	1.318E+10	4.038E+08	3.083E+08	1.549E+01	5.057E+02
	FAROB	/	4.042E+08	2.288E+08	/	5.067E+02
	CROSTAB	1.322E+10	3.804E+08	2.106E+08	1.461E+01	5.070E+02
	Elasticity	1.321E+10	4.042E+08	3.101E+08	1.550E+01	5.067E+02
2/7.5	PreComp	2.200E+10	5.537E+08	3.984E+08	2.127E+01	8.438E+02
	VABS	1.613E+10	4.423E+08	3.386E+08	1.696E+01	6.188E+02
	FAROB	/	4.423E+08	2.154E+08	/	6.193E+02
	CROSTAB	1.616E+10	3.907E+08	3.365E+08	1.501E+01	6.198E+02
	Elasticity	1.615E+10	4.424E+08	3.394E+08	1.697E+01	6.193E+02
1/3	PreComp	2.750E+10	5.936E+08	4.115E+08	2.280E+01	1.055E+03
	VABS	1.834E+10	4.586E+08	3.515E+08	1.759E+01	7.034E+02
	FAROB	/	4.586E+08	1.839E+08	/	7.037E+02
	CROSTAB	1.837E+10	3.669E+08	3.309E+08	1.411E+01	7.046E+02
	Elasticity	1.835E+10	4.587E+08	3.519E+08	1.759E+01	7.037E+02

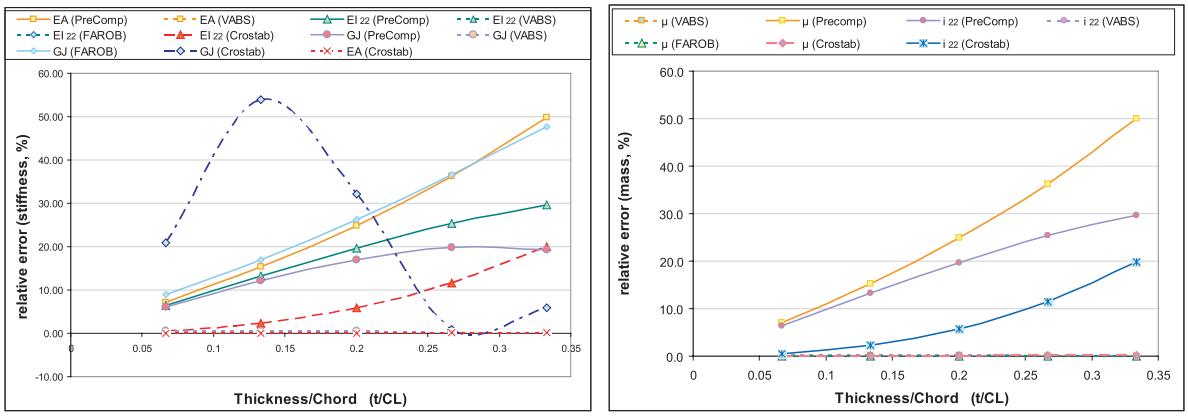

(a) Relative errors in stiffness coefficients (b) Relative errors in mass coefficients

Figure 3. Relative errors in stiffness and mass coefficients with respect to the thickness to diameter ratio.

cross-sectional property evaluated using one of aforementioned tools and X_{exact} is the corresponding exact solution obtained using the Elasticity theory. It can be observed from the plots that both mass and stiffness coefficients obtained by VABS are almost exactly the same as those calculated by the Elasticity theory, with maximum error less than 0.19%. This observation confirms the proof in Yu and Hodges' study[27] that VABS can reproduce the Elasticity theory results for isotropic prismatic beams. The relative errors of these coefficients predicted by PreComp increase as $t/(2R)$ becomes larger, except that the relative errors of the torsional stiffness reaches its peak at $t/(\text{CL}) = 0.26$, then becomes smaller with further increment of $t/(\text{CL})$. FAROB also has an excellent prediction for the bending stiffness and mass per unit length. CROSTAB has an excellent prediction for extensional stiffness and mass per unit length. What surprises the authors are that PreComp results demonstrate large errors even for simple coefficients such as the extensional stiffness EA and mass per unit length μ. This may be attributed to the thin-walled assumption adopted by PreComp, where the cross-sectional area is often approximated by the wall thickness times a characteristic length, e.g., the length of the outer profile curve, the mid curve or the inner arc of the wall. Results obtained by using this approximation will result in larger errors for sections with relatively thick walls. Even $t/(2R)$ is as small as 1/7.5, and PreComp has over 10% error for both stiffness and mass coefficients. It is also strange that errors of the torsional stiffness predicted by CROSTAB reaches more than 50% at $t/(\text{CL}) = 0.13$ and then decreases to zero at $t/(\text{CL}) = 0.26$ and starts to increase again when the tube gets thicker.

For reference, the 6×6 Timoshenko stiffness matrix calculated by VABS for the circular aluminium tube with $t/(2R) = 1/3$ is listed below:

$$\begin{bmatrix} 1.834E+10 & 0.0 & 0.0 & 0.0 & 0.0 & 0.0 \\ & 4.682E+09 & 0.0 & 0.0 & 0.0 & 0.0 \\ & & 4.682E+09 & 0.0 & 0.0 & 0.0 \\ & & & 3.515E+08 & 0.0 & 0.0 \\ & & \textit{symmetry} & & 4.586E+08 & 0.0 \\ & & & & & 4.586E+08 \end{bmatrix}$$

4.2. A highly heterogeneous section

The second example is a highly heterogeneous section (see the left sketch in Figure 4) artificially made from an isotropic channel section (see the right sketch in Figure 4). The isotropic channel is made of a material having $E = 206.843$ GPa, $\nu = 0.49$ and $\rho = 1068.69$ kg/m^3. The rest of the section is made of a fake material with its Young's modulus and density 1.0×10^{-12} times smaller than those of the real material. This provides a challenging test case for cross-sectional tools to handle highly heterogeneous sections. It is expected that the fake material will not provide stiffness and inertia to this section because of its extremely small modulus and density. Hence, the overall properties will be the same as the isotropic channel section, whose analytical solution can be readily obtained using the thin-walled theory. This section is modelled by both PreComp and VABS. PreVABS is used here to generate

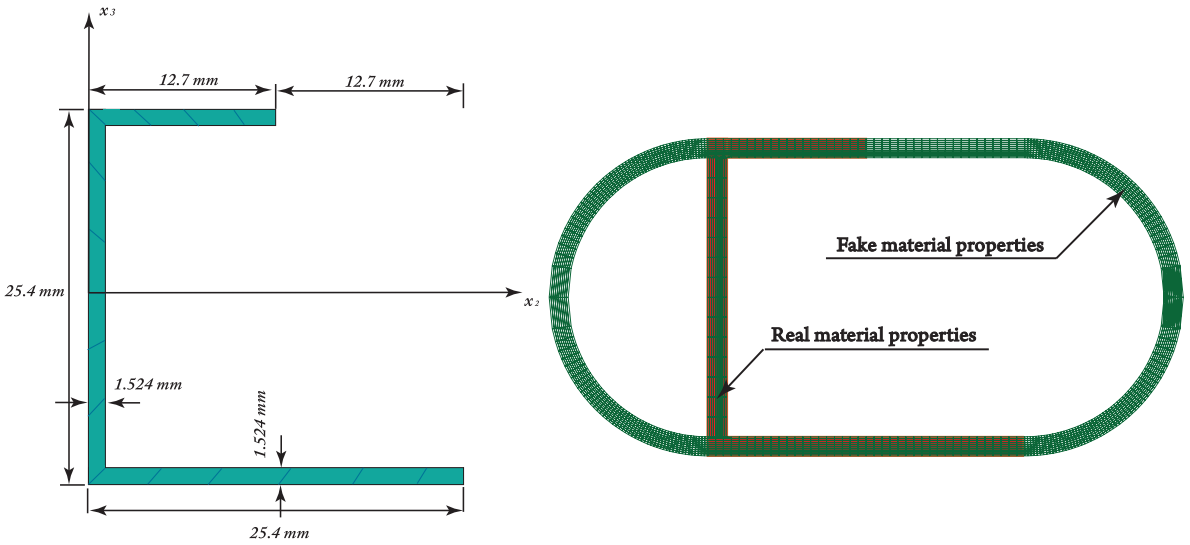

(a) Schematic of an isotropic channel section (b) Schematic of a highly heterogeneous section

Figure 4. Schematic and PreVABS modelling of a channel section

Table II. Sectional properties of the highly heterogeneous section

	PreComp	VABS	Analytical	% Diff. (PreComp)	% Diff. (VABS)
EI_{22}	1.652E+03	2.463E+03	2.463E+03	32.931	0.021
EI_{33}	1.543E+04	3.510E+03	3.542E+03	335.670	0.903
GJ	5.318E–08	4.952	4.918	100	0.691
EA	2.0020E+07	1.9045E+07	1.9056E+07	5.058	0.060
S_{34}	–1.385E+03	–6.132E+02	–6.263E+02	121.153	2.079
S_{13}	–3.186E+04	1.042E+05	1.053E+05	130.261	1.005
S_{14}	2.464E+05	–2.176E+05	–2.191E+05	212.439	0.686
μ	0.103	9.840E–02	9.846E–02	5.020	0.060
i_{22}	7.806E–06	3.781E–06	3.783E–06	106.336	0.065
i_{33}	6.451E–05	1.124E–05	1.125E–05	473.571	0.050
x_{m2}	–2.000E–03	6.956E–03	6.952E–03	128.769	0.053
x_{m3}	–2.000E–03	–2.509E–03	–2.508E–03	20.255	0.027
x_{s2}	1.100E–02	–4.472E–03	–4.548E–03	341.874	1.665
x_{s3}	–4.000E–03	–7.981E–03	–8.004E–03	50.027	0.286
θ	–5.212	–26.580	–26.588	80.397	0.030

the cross-sectional meshes and the input files for VABS. However, it is worthy to note that VABS is not limited to closed sections, as shown by the same section analysed directly without help of the fake material in Yu and Hodges'[17] study. The cross-section is meshed as follows: (i) both for PreVABS and PreComp, 10 layers are used for through-thickness discretization; (ii) 120 and 280 segments are used for PreComp and PreVABS, respectively, for meshing the elliptic circumference. The reason why only 120 segments are used for PreComp modelling is because when more segments are used in PreComp, an unknown error is generated. The results obtained by PreComp, VABS and thin-walled theory are listed in Table II. It is noted that FAROB and CROSTAB are not used to analyse this section because of difficulties modelling this section in these two codes. In Table II, θ represents the angle in degrees rotating from x_2 to the principal inertial axis around the positive x_1 direction. The relative differences are calculated with respect to the analytical results.

It can be observed that for this section, results predicted by VABS match well with those of the analytical results based on the thin-walled theory, with the maximum percentage difference (2.079%) occurring for the coupling bending stiffness (S_{34}). Since this section is indeed a thin-walled section, it is not a surprise that analytical results based on the thin-walled theory match VABS results very well. However, PreComp results exhibit very large relative difference on literally all sectional properties except extensional stiffness (EA) and mass per unit length (μ). Particularly, the prediction on torsional stiffness GJ by PreComp is nowhere near the theoretical value, indicating that PreComp is not suitable for analysing

highly heterogeneous cross-sections if the material properties between different segments of the blade section are drastically different. The 6 × 6 Timoshenko stiffness matrix for the highly heterogeneous section is:

$$\begin{bmatrix} 1.903E+07 & 0.0 & 0.0 & 0.0 & -4.778E+04 & -1.325E+05 \\ & 2.791E+06 & 2.364E+05 & 2.122E+04 & 0.0 & 0.0 \\ & & 2.137E+06 & -7.679E+03 & 0.0 & 0.0 \\ & & & 2.086E+02 & 0.0 & 0.0 \\ & & \textit{symmetry} & & 2.010E+03 & 9.102E+02 \\ & & & & & 1.944E+03 \end{bmatrix}$$

4.3. A multi-layer composite pipe

The third example is a multi-layer composite pipe with the geometry and the lamination information shown in Figure 5. It is a thin-walled cross-section with the thickness of wall to the chord length ratio is less than 0.1. Each layer is made of composite materials having properties as E_{11} = 141.963 GPa, $E_{22} = E_{33}$ = 9.79056 GPa, $G_{12} = G_{13} = G_{23}$ = 59.9844 GPa and $\nu_{12} = \nu_{13} = \nu_{23}$ = 0.42. Both VABS and PreComp use 20 layers for through-thickness discretization and 143 segments for discretization along the circumference. The stiffness coefficients predicted by PreComp, VABS, FAROB, CROSTAB and SVBT (Saint Venant Beam Theory) are listed in Table III, where the relative differences are calculated with respect to SVBT. SVBT is a computer program based on the theory developed in Giavott *et al.*'s,[28] a theory developed in Italian helicopter industry using the generalized Saint-Venant approach. SVBT only produces the stiffness matrix for a generalized Timoshenko model. The corresponding stiffness coefficients for the Euler–Bernoulli model can be obtained by inverting the remaining 4 × 4 matrix of the flexibility matrix of the generalized Timoshenko model after eliminating the two rows and two columns corresponding to the transverse shears. The relative differences are calculated with respect to the SVBT results. Mass

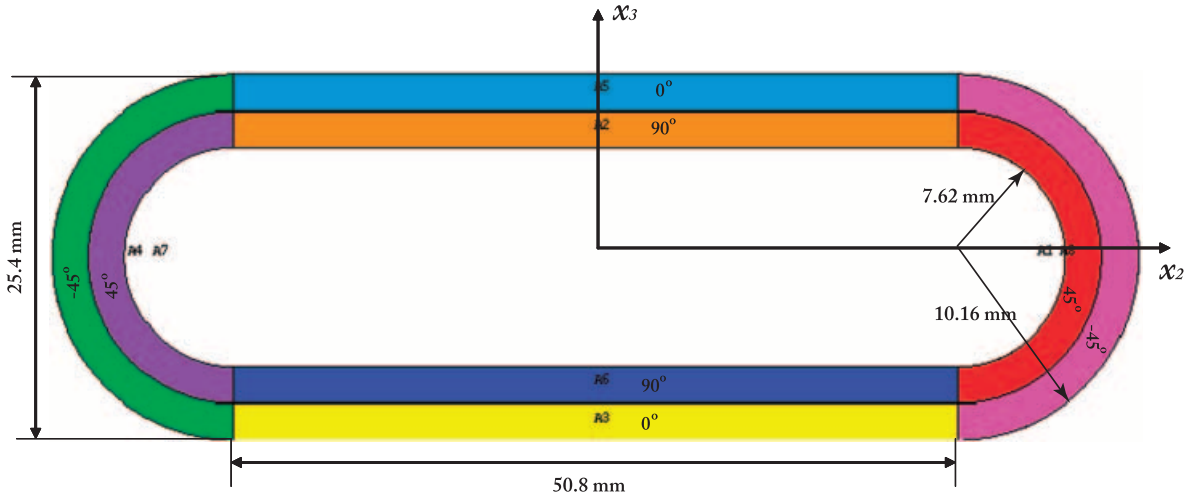

Figure 5. Schematic of a composite elliptical pipe.

Table III. Stiffness coefficients of the multilayered composite pipe.

Variables	EI_{22}	EI_{33}	GJ	EA	S_{12}
PreComp	7.074E+03	4.857E+04	8.628E+03	7.833E+07	−1.205E−02
VABS	5.402E+03	1.547E+04	1.972E+03	4.621E+07	1.111E+04
FAROB	6.182E+03	2.297E+04	4.240E+03	/	/
CROSTAB	6.694E+03	4.012E+04	1.500E+01	7.000E+07	0.0
SVBT	5.402E+03	1.547E+04	1.972E+03	4.621E+07	1.112E+04
% Diff. (PreComp)	30.950	214.005	337.447	69.499	100.000
% Diff. (VABS)	0.001	0.003	0.044	0.0004	0.172
% Diff. (FAROB)	14.429	48.485	114.974	/	/
% Diff. (CROSTAB)	23.906	159.363	99.240	51.465	100%

coefficients are not provided because they are not available from SVBT. Because of the symmetry, centroid and generalized shear centre coincides with the origin of the coordinate system. It can be observed from Table III that the VABS results show an excellent agreement with the SVBT results (with the maximum relative difference less than 0.5%). The results calculated by PreComp, FAROB and CROSTAB demonstrate large deviations, with the prediction of PreComp being the worst, particularly for the torsional stiffness GJ and the bending stiffness EI_{33}. None of these three tools (PreComp, FAROB and CROSTAB) can predict the significant extension-twist coupling, S_{12}, for this section, although this coupling is almost five times of the torsional stiffness. This is because the accuracy of the sectional properties of anisotropic and heterogeneous sections is strongly dependent on an accurate calculation of the warping functions. Methods based on *a priori* assumptions for the section to warp in a certain fashion or completely neglecting the warping effect will have a hard time to provide an accurate prediction for the sectional properties.

The 6×6 Timoshenko stiffness matrix for the multilayer composite pipe section is listed as follows:

$$\begin{bmatrix} 4.621E+07 & 0.0 & 0.0 & 1.111E+04 & 0.0 & 0.0 \\ & 3.489E+06 & 0.0 & 0.0 & -9.251E+02 & 0.0 \\ & & 1.463E+06 & 0.0 & 0.0 & -5.859E+03 \\ & & & 1.971E+03 & 0.0 & 0.0 \\ & & \textit{symmetry} & & 5.402E+03 & 0.0 \\ & & & & & 1.547E+04 \end{bmatrix}$$

4.4. An Isotropic blade-like section

The previous three cross-sections have very simple geometry. It will be interesting to find out how different methods perform for more complex geometry, particularly, rotor blade like geometry, which are the target applications of all the tools we are currently assessing. To this end, we suggest an isotropic blade-like section as shown in Figure 6. It is noted that the inclined straight edges at the tail are tangent to the ending arc at the head. Material properties of this section are the same as the channel in Figure 4. Both for VABS and PreComp, 10 layers are used for cross-thickness discretization, while 120 segments are used for meshing the blade-like circumference.

The predictions of sectional properties by PreComp, VABS, CROSTAB, the sectional capability of ANSYS and analytical results based on the thin-walled theory are listed in Table IV. Since FAROB only provides very limited information it is not meaningful to compare it with other tools for this example. All the stiffness properties are given in a coordinate system with the origin located at the shear centre and x_2 and x_3 axes parallel to the axes sketched in Figure 6. It is pointed out that CROSTAB outputs stiffness coefficients with respect to the tension centre and the shear centre location is not calculated. To facilitate our comparison, VABS shear centre location is used to convert CROSTAB stiffness results to be in the same coordinate system as used by VABS. For all the other

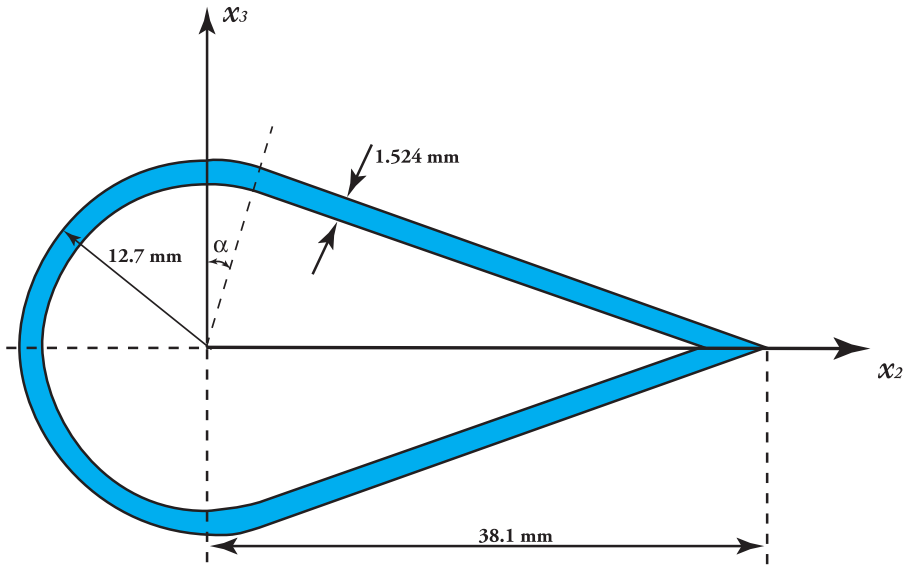

Figure 6. Schematic of an isotropic blade-like section.

Table IV. Sectional properties of an isotropic blade-like section.

	PreComp	VABS	CROSTAB	Analytical	ANSYS
EI_{22}	2.178E+03	2.101E+03	1.963E+03	2.101E+03	2.101E+03
EI_{33}	9.100E+03	1.050E+04	1.153E+04	1.110E+04	1.051E+4
GJ	1.696E+03	1.760E+03	1.977E+03	1.706E+03	1.760E+03
EA	3.794E+07	3.566E+07	3.700E+07	3.567E+07	3.567E+07
S_{14}	–3.238E–02	–3.046E+05	0.0	–3.379E+05	–3.051E+05
μ	1.960E–01	1.843E–01	1.912E–01	1.843E–01	1.843E–01
i_{22}	1.125E–05	1.085E–05	1.014E–05	1.085E–05	1.085E–05
i_{33}	4.702E–05	4.080E–05	4.564E–05	4.081E–05	4.081E–05
x_{m2}	1.000E–02	9.516E–03	1.045E–02	9.513E–03	9.513E–03
x_{t2}	1.000E–02	9.516E–03	1.045E–02	9.513E–03	9.513E–03
x_{s2}	1.000E–02	9.75E–04	/	3.90E–05	9.59E–04

Table V. Differences of sectional properties of an isotropic blade-like section.

	% Diff. (PreComp)	% Diff. (CROSTAB)	% Diff. (Anal.)	% Diff. (ANSYS)
EI_{22}	3.663	6.581	0.017	0.016
EI_{33}	13.348	9.824	5.701	0.065
GJ	3.618	12.345	3.062	0.004
EA	6.386	3.753	0.015	0.014
S_{14}	100.0	100.0	10.943	0.166
μ	6.373	3.754	0.015	0.015
i_{22}	3.697	6.525	0.043	0.044
i_{33}	15.246	11.874	0.026	0.026
x_{m2}	5.090	9.861	0.029	0.030
x_{t2}	5.090	9.861	0.029	0.030
x_{s2}	926.100	/	96.039	1.639

results, the stiffness results are given in terms of their own shear centre locations.

The differences between various approaches are listed in Table V, where the relative differences are calculated with respect to the VABS results. Among all the methods, VABS results are the closest to the values predicted by ANSYS, with the maximum difference between these two methods being 1.639%. While the analytical method based on the thin-walled theory provides an accurate prediction of mass moments of inertia as well as the tensional stiffness, torsional stiffness and bending stiffness EI_{22}, it demonstrates relative larger errors on predicting the extension-bending coupling S_{14} and the bending stiffness EI_{33}. This is attributed to the fact that the analytical approach based on the thin-walled theory cannot accurately locate the shear centre. For example, the analytically predicted value of $x_{sc} = 0.000039$ m is far less than the VABS result (0.000975 m) and that of ANSYS (0.000959 m). The results predicted by PreComp and CROSTAB are even worse. For example, shear centre $x_{sc} = 0.01000$ m predicted by PreComp, is far larger than the VABS as well as ANSYS values. Neither PreComp nor CROSTAB can predict the significant extension-bending coupling S_{14}. It is a thin-walled structure with a wall-thickness-to-chord-length ratio of 0.03, for which one might expect the thin-walled theory, PreComp and CROSTAB to have a relative good performance. However, this example shows that this is not the case. The 6×6 Timoshenko stiffness matrix for the isotropic blade-like section is listed below for reference:

$$\begin{bmatrix} 3.566E+07 & 0.0 & 0.0 & 0.0 & 0.0 & -3.394E+05 \\ & 8.252E+06 & 0.0 & 0.0 & 0.0 & 0.0 \\ & & 2.444E+06 & 2.382E+03 & 0.0 & 0.0 \\ & & & 1.762E+03 & 0.0 & 0.0 \\ & & \textit{symmetry} & & 2.101E+03 & 0.0 \\ & & & & & 1.113E+04 \end{bmatrix}$$

4.5. A realistic wind turbine blade

To complete our assessment, two cross-sections at different spanwise stations of a realistic composite wind turbine blade with five varying skin segments and two webs are analysed and compared using PreComp, VABS and CROSTAB. A schematic of a typical wind turbine blade cross-section as well as coordinate systems is depicted in Figure 7. An MH 104 airfoil for stall controlled wind turbines is used (http://www.ae.illinois.edu/m-selig/ads/coord-database.html). The cross-sectional characteristic geometric data such as the chord length, the twist angle, the pitch axis location, the web location, the x_2 coordinate of representative points for defining the skin segments as well as the material properties for different laminated materials are provided in Table VI, where the elastic and shear moduli have the units of Pa and the material density ρ has the unit of kg/m^3. The detailed lamination information for

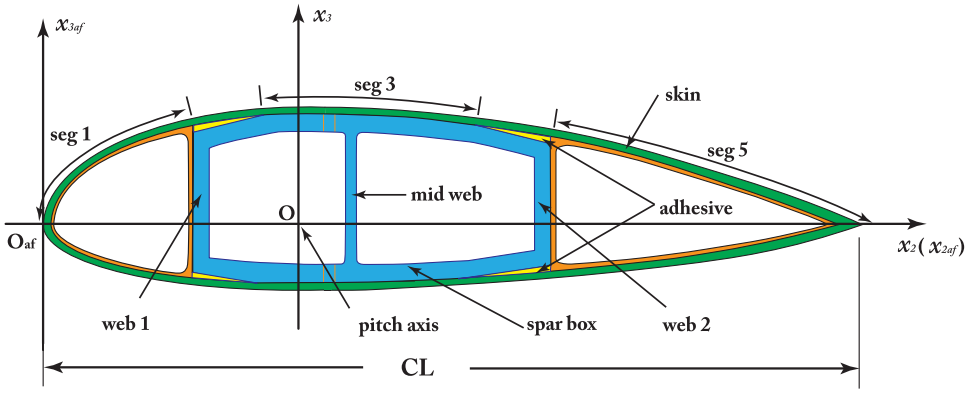

Figure 7. Sketch of a cross-section for a typical wind turbine blade.

Table VI. Geometric data and material properties of the wind turbine blade sections at two different stations.

Blade characteristic geometric data						
	Chord length	Twist angle	Pitch axis[a]		Web centre-line[b]	
	CL	θ	x_{p2}	x_{p3}	Web 1	Web 2
st1	1.9000	0.0000	0.4750	0.0000	0.15	0.5
st2	0.4540	0.0000	0.1135	0.0000	0.15	0.5
Non-dimensional coordinates of representative nodes on the cross-sectional airfoil profile[c]						
	$x1$	$x2$	$x3$	$x4$	$x5$	$x6$
st1	0.0000	0.0016	0.0041	0.1147	0.5366	1.0000
st2	0.0000	0.0016	0.0041	0.0839	0.5366	1.0000
3D material properties[d]						
material name	material ID	E_{11}	$E_{22} = E_{33}$	$G_{12} = G_{13} = G_{23}$	$\nu_{12} = \nu_{13} = \nu_{23}$	ρ
uni-directional FRP	1	3.70E+10	9.00E+09	4.00E+09	0.28	1.860E+03
double-bias FRP	2	1.03E+10	1.03E+10	8.00E+09	0.30	1.830E+03
Gelcoat	3	10.00	10.00	1.00	0.30	1.830E+03
Nexus	4	1.03E+10	1.03E+10	8.00E+09	0.30	1.664E+03
Balsa	5	1.00E+07	1.00E+07	2.00E+05	0.30	1.280E+02

[a] coordinates of the pitch axis measured in the blade's airfoil coordinate system, see Figure 7.
[b] Non-dimensional x_2 coordinate of the centre-line of each web measured in the blade's airfoil coordinate system, divided by the chord length. There are two webs each in the selected cross-sections and these webs are all perpendicular to the chord line.
[c] x_2/CL of representative points on the airfoil profile of each cross-section for dividing the top and bottom skins into several specified segments. For the present analysis, the bottom skin's laminate lay-up configuration is a mirror image of that of the top.
[d] To facilitate our comparison between VABS and PreComp, 2D material properties obtained from a PreComp example on analysing a real wind turbine blade[12] are expanded to their 3D counterparts.
FRP, Fibre Reinforced Plastics.

the two cross-sections is listed in Table VII. It is worthy to note that this section has the full elastic coupling between extension, twist and bending including extension-twist coupling (S_{12}), extension-bending couplings (S_{13}, S_{14}) the twist-bending couplings (S_{23}, S_{24}) and bending-bending coupling S_{34}. These couplings for this realistic composite wind turbine blade are significant and they should be calculated accurately for a reliable prediction of the aeroelastic dynamic behaviour of the wind turbine system.

For VABS analysis, PreVABS is used as an automatic modelling tool to generate the finite element model for the cross-section. For the cross-section at station 1 (st1), 86,736 nodes and 85,945 quadrilateral and triangular elements are generated and detailed lamination information necessary for VABS analysis such as the ply titling angle θ_1 and the fibre orientation angle θ_3 are calculated for each element. The finite element model generated for cross-section st1 is plotted in Figure 8. It should be noted

Table VII. Laminate layup schema for the wind turbine blade sections at two different stations.

Component name	Number of plies	layer thickness	Fibre orientation angle	Material ID
Laminate layer schema for station 1				
Segments 1 & 2	1	0.000381	0	3
	1	0.00051	0	4
	18	0.00053	20	2
Segment 3	1	0.000381	0	3
	1	0.00051	0	4
	33	0.00053	20	2
Segment 4	1	0.000381	0	3
	1	0.00051	0	4
	17	0.00053	20	2
	38	0.00053	30	1
	1	0.003125	0	5
	37	0.00053	30	1
	16	0.00053	20	2
Segment 5	1	0.000381	0	3
	1	0.00051	0	4
	17	0.00053	20	2
	1	0.003125	0	5
	16	0.00053	0	2
Webs 1 & 2	38	0.00053	0	1
	1	0.003125	0	5
	38	0.00053	0	1
Laminate layer schema for station 2				
Segments 1 & 2	1	0.000381	0	3
	1	0.00051	0	4
	3	0.00053	20	2
Segment 3	1	0.000381	0	3
	1	0.00051	0	4
	8	0.00053	20	2
Segment 4	1	0.000381	0	3
	1	0.00051	0	4
	4	0.00053	20	2
	9	0.00053	30	1
	1	0.003125	0	5
	9	0.00053	30	1
	4	0.00053	20	2
Segment 5	1	0.000381	0	3
	1	0.00051	0	4
	4	0.00053	20	2
	1	0.003125	0	5
	4	0.00053	0	2
Webs 1 & 2	16	0.00053	0	1
	1	0.003125	0	5
	16	0.00053	0	1

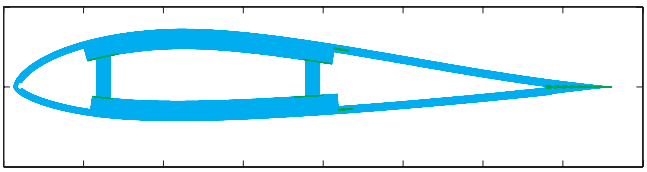

Figure 8. Finite element discretization of cross-section at station 1 generated by PreVABS. This figure represents a particular design of the blade cross-section specified by the data provided in Tables VI and VII and is slightly different from the generic section depicted in Figure 7.

Table VIII. Sectional properties of the wind turbine blade section at station 1.

	PreComp	CROSTAB	VABS	% Diff. (PreComp)	% Diff. (CROSTAB)
EI_{22}	2.103E+07	1.459E+08	1.916E+07	9.778	661.734
EI_{33}	6.309E+08	4.878E+08	4.398E+08	43.448	10.907
GJ	1.008E+07	2.469E+07	2.167E+07	53.479	13.950
EA	3.000E+09	2.789E+09	2.387E+09	25.664	16.826
S_{34}	–8.132E+06	6.010E+07	1.210E+07	167.204	396.632
S_{13}	–1.037E+06	5.216E+08	–2.635E+07	96.065	2.079E+03
S_{14}	–1.301E+08	1.685E+08	–4.724E+08	72.459	135.671
S_{23}	–3.776E+05	9.002E+09	–5.222E+04	623.105	1.724E+07
S_{24}	8.746E+06	–1.208E+09	1.422E+06	514.904	8.504E+04
S_{12}	7.522E+05	–1.723E+09	–3.381E+07	102.225	4.996E+03
μ	285.9	289.132	258.053	10.791	12.044
i_{22}	2.211	5.144	2.172	1.797	136.837
i_{33}	62.72	61.340	46.418	35.121	32.148
x_{m2}	0.332	0.284	0.27780	19.444	2.064
x_{m3}	0.027	–0.028	0.02743	1.572	201.272
x_{t2}	0.331	–0.0290	0.233	42.173	112.466
x_{t3}	0.028	0.2273	0.029	3.287	685.174
x_{s2}	0.287	/	0.031	813.479	/
x_{s3}	0.028	/	0.040	30.478	/
θ	–0.990	3.7919	–1.244	20.419	404.813

Table IX. Sectional properties of the wind turbine blade section at station 2.

Variables	PreComp	CROSTAB	VABS	% Diff. (PreComp)	% Diff. (CROSTAB)
EI_{22}	6.363E+04	8.608E+05	5.878E+04	8.253	1.364E+03
EI_{33}	2.784E+06	2.481E+06	1.586E+06	75.570	56.487
GJ	4.103E+04	9.379E+04	7.027E+04	41.613	33.473
EA	2.090E+08	2.115E+08	1.533E+08	36.375	38.026
S_{34}	–2.149E+04	2.433E+05	4.159E+04	151.669	485.000
S_{13}	–1.558E+04	1.187E+07	–4.297E+05	96.374	2.861E+03
S_{14}	–7.272E+06	1.332E+06	–7.224E+06	0.662	118.444
S_{23}	–9.178E+02	1.671E+07	1.214E+02	856.218	1.376E+07
S_{24}	1.833E+04	–4.429E+06	6.274E+03	192.172	7.070E+04
S_{12}	4.719E+03	–3.037E+07	–1.314E+04	135.911	2.310E+05
μ	20.050	22.07	16.763	19.609	31.679
i_{22}	7.229E–03	0.0208	7.017E–03	3.025	196.177
i_{33}	0.2644	0.318	0.174	52.144	82.918
x_{m2}	0.089	0.0871	0.0619	43.672	40.624
x_{m3}	0.006	–0.0040	0.0065	7.523	161.436
x_{t2}	0.092	–0.0051	0.0492	86.860	110.359
x_{t3}	0.007	0.0659	0.0069	1.722	857.642
x_{s2}	0.058	/	0.0012	4.719E+03	/
x_{s3}	0.007	/	0.0098	28.210	/
θ	–0.8490	4.210	–1.117	24.023	476.620

here that the finite element model of the cross-section depicted in Figure 8 is slightly different from the section plotted in Figure 7 as Figure 7 represents a generic design of a wind turbine blade cross-section and Figure 8 represents a particular design of the blade cross-section specified by the data provided in Table VI and VII. To facilitate our comparison, both VABS and PreComp use the same lamina layup schema listed in Table VII and 124 segments (maximum limit for PreComp) along the blade circumference. Resulting cross-sectional properties for st1 and station 2 (st2) are presented in Tables VIII and IX, respectively, with the relative differences (errors) calculated with respect to the VABS results. From Table VIII, it can be observed that while the differences of PreComp and VABS are relatively small (below 10%) for EI_{22}, i_{22}, x_{m3} and x_{t3}, all the other sectional properties have significant differences. Particularly, huge differences (over 100%) exist for the shear centre location in the x_2 direction, mass moment of inertia i_{33} and most of the coupling stiffness terms. Similar observations can be found for cross-section at st2, which having a shorter chord length and thinner composite layers except for this section, both PreComp and VABS

predict almost the same S_{14}. As far as the difference between CROSTAB and VABS are concerned, the relative errors for CROSTAB are, in general, larger than those of PreComp. The relative differences between CROSTAB and VABS are relatively small (below 20%) for EI_{33}, EA, GJ, x_{m2} and μ for st1 section and all relative error are larger than 30% for the st2 section. Huge differences (over 100%) exist for bending stiffness EI_{22}, mass moment of inertia i_{22}, mass centre location x_{m3}, x_{t2} and x_{t3}. Extremely large errors (over 1000%) occur for most of the coupling stiffness terms. The results predicted by PreComp and CROSTAB are also very different between each other. For example, comparing the values commonly used for a blade simulation, one can find PreComp predicts better for EI_{22}, i_{22}, x_{m3} and x_{t3}, while CROSTAB performs better for EI_{33}, EA and GJ.

The 6×6 Timoshenko stiffness matrix for the realistic composite wind turbine blade at station 2 is listed below for reference:

$$\begin{bmatrix} 2.389E+09 & 1.524E+06 & 6.734E+06 & -3.382E+07 & -2.627E+07 & -4.736E+08 \\ & 4.334E+08 & -3.741E+06 & -2.935E+05 & 1.527E+07 & 3.835E+05 \\ & & 2.743E+07 & -4.592E+04 & -6.869E+02 & -4.742E+06 \\ & & & 2.167E+07 & -6.279E+04 & 1.430E+06 \\ & & \textit{symmetry} & & 1.970E+07 & 1.209E+07 \\ & & & & & 4.406E+08 \end{bmatrix}$$

5. DISCUSSIONS

From all these examples, VABS has demonstrated consistent and reliable predictions for all the material properties in comparing to the Elasticity theory, analytical results based on thin-walled theory, and other well-accepted tools including ANSYS and SVBT. However, such consistency is not found for PreComp, FAROB and CROSTAB. When the cross-section is an isotropic, homogeneous closed section with simple geometry, such as the circular aluminium tube, and when the wall thickness is small compared with the dimension of the cross section, PreComp, FAROB and CROSTAB can provide a reasonable prediction for the inertial and structural properties, except for the CROSTAB prediction of torsional stiffness which cannot be trusted. The errors becomes larger as the wall gets thicker, although FAROB remains the perfect prediction for bending stiffness and mass per unit length and CROSTAB remains the perfect prediction for the extensional stiffness and mass per unit length. When the isotropic homogenous, closed-section becomes more complex in geometry, such as the isotropic blade-like section, the prediction of PreComp and CROSTAB becomes worse, particularly for the shear centre prediction and coupling stiffness coefficients. For highly heterogenous sections such as the isotropic channel section, even if they are very thin, PreComp cannot provide reliable predictions for most of the properties except the extensional stiffness and mass per unit length. For sections made of anisotropic materials, such as the multi-layer composite pipe, the predictions of PreComp, FAROB and CROSTAB have huge differences comparing the results of VABS and SVBT, and some of the coupling terms cannot be predicted by these three tools. It is also worthy to note that predictions made by PreComp, FAROB and CROSTAB vary with big differences when compared with each other, although they are all implementations of analytical formulas based on a similar theoretical foundation and are common tools currently used by wind turbine engineers. As the wind turbine blades get more and more sophisticated, real wind blade sections, such as the one in Figure 7, will become highly heterogeneous and highly anisotropic. A cross-sectional tool with solid mathematical foundation and demonstrated performance, such as VABS, should be used to accurately predict the sectional properties which are crucial for dynamic and aeroelastic simulations of the complete wind turbine system so that high-performance systems can be designed and build more cost effectively.

6. CONCLUSIONS

In this paper, we have critically assessed several computer tools commonly used for calculating wind turbine blade properties including PreComp, VABS, FAROB, CROSTAB and BPE. The meaning of sectional properties including both inertial and structural properties is precisely described, and the transformation of the sectional properties to a different coordinate system is clearly specified. The theoretical foundation of each tool is briefly summarized and the advantages and disadvantages of each tool are pointed out. Several benchmark examples are used to evaluate the performance of different tools and huge differences have been found among these wind turbine blade tools. We have also observed that only VABS consistently provides reliable predictions for all the cross-sections we have tested. Such a systematic and critical assessment should provide some guidance for engineers to choose the right tool to effectively design and analyse wind turbine blades with confidence. Because of the poor, and inconsistent performance of PreComp, FAROB, and CROSTAB for simple cross-sections, their applicability to real complex, composite wind turbine blades is questionable. On the other hand,

through this assessment, VABS, a proven technology in helicopter industry, demonstrates its clear advantage and performance over other tools. Particularly empowered with PreVABS, one should be able to use VABS to perform an efficient yet accurate modelling of the wind turbine blades with nominal human interaction efforts not more than PreComp, FAROB or CROSTAB. This assessment paper also points out that we need to provide a more extensive validation of the computational tools currently being used in the wind industry.

ACKNOWLEDGEMENTS

This research was supported in part by the Army Vertical Lift Research Center of Excellence at Georgia Institute of Technology and its affiliate programme through subcontract at Utah State University. The technical monitor is Dr. Michael J. Rutkowski. The results of FAROB and CROSTAB are generated independently by the third author and all other results are generated by the first two authors.

REFERENCES

1. Laird DL. Wind energy industry overview. *Proceedings of the 2008 Wind Turbine Blade Workshop*, Sandia National Laboratories, Albuquerque, New Mexico, May 12–14 2008.
2. Veers PS, Ashwill TD, Sutherland HJ, Laird DL, Lobitz DW. Trends in the design, manufacture and evaluation of wind turbine blades. *Wind Energy* 2003; **6**: 245–259.
3. Laird DL, Montoya FC, Malcolm DJ. Finite element modeling of wind turbine blades. *Collection of the 2005 ASME Wind Energy Symposium Technical Papers at the 43rd AIAA Aerospace Sciences Meeting and Exhibit*, Reno, NV, United States, 2005; 9–17.
4. Pardo DR, Kim B. Finite element analysis of the cross-section of wind turbine blades: a comparison between shell and 2D-solid models. *Wind Engineering* 2005; **29**: 25–32.
5. Laird DL Ashwill T. Introduction to NuMAD: a numerical manufacturing and design tool. *Proceedings of the AIAA/ASME Wind Energy Symposium*, AIAA, Reno, Nevada, January 1998; 354–360.
6. Malcolm DJ, Laird DL. Extraction of equivalent beam properties from blade models. *Wind Energy* 2007; **10**: 135–157.
7. Lee D, Hodges DH, Patil MJ. Multi-flexible-body dynamic analysis of horizontal axia wind turbines. *Wind Energy* 2002; **5**: 281–300.
8. Yu W. Efficient high-fidelity simulation of multibody systems with composite dimensionally reducible components. *Journal of the American Helicopter Society* 2007; **52**: 49–57.
9. Hodges DH. *Composite Nonlinear Theory.* AIAA: Reston, VA, 2006.
10. Yu W, Hodges DH. Best strip-beam properties that are derivable from Classical Lamination Theory. *AIAA Journal* 2008; **46**: 1719–1724.
11. Bir G. Computerized Method for preliminary structural design of composite wind turbine blades. *Journal of Solar Energy Engineering* 2001; **123**: 372–381.
12. Bir GS. User's guide to PreComp (pre-processor for computing composite blade properties). Technical Report NREL/TP-500-38929. *National Renewal Energy Laboratory* 2006
13. Philippidis TP, Vassilopoulos AP, Katopis KG, Voutsinas SG. THIN/PROBEAM: a software for fatigue design and analysis of composite rotor blades. *Wind Engineering* 1996; **20**: 349–362.
14. Lindenburg C. STABLAD-stability analysis tool for anisotropic rotor blade panels). Technical Report ECN-CX–99-031 r1. *Energy Research Center of the Netherlands* 2008
15. Yu W. Variational asymptotic modeling of composite dimensionally reducible structures. PhD Thesis, Aerospace Engineering, Georgia Institute of Technology, May 2002.
16. Hodges DH, Yu W. A rigorous, engineering-friendly approach for modeling realistic, composite rotor blades. *Wind Energy* 2007; **10**: 179–193.
17. Yu W, Hodges DH. Generalized Timoshenko theory of the variational asymptotic beam sectional analysis. *Journal of the American Helicopter Society* 2005; **50**: 46–55.
18. Ku J, Volovoi VV, Hodges DH. Multilevel-Multiphase Optimization of Composite Rotor Blade with Surrogate Model. *Proceedings of the 48th Structures, Structural Dynamics, and Materials Conference*, AIAA, Honolulu, Hawaii, April 23–26 2007.
19. Lindenburg C, Hegberg T. PHATAS-IV user's manual: program for Horizontal axis wind turbine analysis and simulation, version IV. Technical Report ECN-C–99-093. *Energy Research Center of the Netherlands* 2000
20. Yu W, Hodges DH, Volovoi VV, Cesnik CES. On Timoshenko-like modeling of initially curved and twisted composite beams. *International Journal of Solids and Structures* 2002; **39**: 5101–5121.
21. Roy S, Yu W, Han D. An asymptotically correct classical model for smart beams. *International Journal of Solids and Structures* 2007; **44**: 8424–8439.

22. Roy S, Yu W. Dimensional reduction of an end-electroded piezoelectric composite rod. *European Journal of Mechanics—A/Solids*, 2008; **28**: 368–376.
23. Roy S, Yu W. A coupled Timoshenko model for smart slender structures. *International Journal of Solids and Structures* 2009; **46**: 2547–2555.
24. Wang Q, Yu W. Variational asymptotic modeling of the thermal problem of composite beams. *Proceedings of the 50th Structures, Structural Dynamics and Materials Conference*, AIAA, Palm Springs, California, May 4–7 2009.
25. Malcolm DJ, Laird DL. Modeling of blades as equivalent beams for aeroelastic analysis. *Proceedings of the AIAA/ASME Wind Energy Symposium*, AIAA, Reno, NV, January 2003.
26. Sun CT. *Mechanics of Aircraft Structures* (1st edn). John Willey & Sons Inc.: New York, US, 1998.
27. Yu W, Hodges DH. Elasticity solutions versus asymptotic sectional analysis of homogeneous, isotropic, prismatic beams. *Journal of Applied Mechanics* 2004; **71**: 15–23.
28. Giavott V, Borri M, Mantegazza P, Ghiringhelli G, Carmaschi V, Maffioli GC, Mussi F. Anisotropic beam theory and applications. *Computers and Structures* 1983; **16**: 403–413.